Advances in Computer, Signals and Systems (2026)
Clausius Scientific Press, Canada

DOI: 10.23977/acss.2026.100116
ISSN 2371-8838 Vol. 10 Num. 1

Midsurface Extraction of Variable-Thickness Thin-Walled Parts Using an Oriented Signed Distance Field

Jiahong Zhang

School of Optical-Electrical and Computer Engineering, University of Shanghai for Science and Technology, Shanghai, 200093, China

Keywords: Mid-surface abstraction; oriented signed distance field; variable-thickness thin-walled models

Abstract: Mid-surface extraction of thin-walled parts is a key technique for CAD dimensional reduction modeling and structural analysis. Particularly for variable-thickness structures, traditional offset-based methods struggle to generate stable and topologically correct mid-surface models. To address this issue, this paper proposes an automatic mid-surface extraction method for variable-thickness thin-walled parts based on an oriented signed distance field (SDF). First, the SDF of the model is constructed, and local minimum points are extracted to form a set of mid-surface candidate points. Subsequently, ray-casting–based face pairing relationships are employed to group matched face pairs. On this basis, geometric consistency filtering is performed using distance symmetry and normal opposition constraints to refine the mid-surface points. For constant-thickness and variable-thickness regions, offset generation and boundary-constrained surface fitting strategies are adopted, respectively, to complete mid-surface reconstruction. Experimental results demonstrate that the proposed method achieves good stability and geometric accuracy across models with different thickness characteristics.

1. Introduction

Thin-walled components are extensively utilized in aerospace, automotive manufacturing, and precision equipment industries, typically exhibiting structural characteristics such as large dimensional spans, significant local curvature variations, and relatively thin walls. To reduce computational complexity in finite element analysis and process planning, engineering practices often require dimensionality reduction of three-dimensional solid models to intermediate surface models for analysis. However, practical thin-walled components frequently exhibit variable thickness features, resulting in highly complex spatial configurations and topological connections of intermediate surfaces. This poses challenges for automatic intermediate surface extraction, including difficulties in ensuring topological continuity and insufficient local positioning accuracy.

Current mid-plane extraction methods predominantly employ geometric strategies such as central axis transformation, equidistant offsetting, and global minimum distance criteria. These approaches typically assume uniform thickness assumptions, which may lead to mid-plane displacement, fractures, and erroneous connections under variable thickness structures or complex topological conditions.

To address the aforementioned challenges, this study proposes an automated median extraction method for variable-thickness thin-walled components based on directed symbolic distance fields. By constructing model-based directed symbolic distance fields and identifying local minimum points, the approach integrates face-to-face matching relationships with geometric consistency constraints to achieve stable recognition and optimized fitting of median candidate points. This methodology effectively enhances positioning accuracy and topological integrity of midplanes in variable-thickness thin-walled structures while maintaining computational efficiency.

2. Related work

Although mid-plane extraction techniques have been extensively studied, they still face numerous challenges in ensuring topological connectivity accuracy and geometric precision. This makes the process of constructing mid-plane models from 3D solid models remain highly dependent on manual intervention in engineering practice. Existing methods can generally be categorized into two major types: geometric methods and mesh methods.

The geometric methods mainly include the central axis method, chord axis method and surface matching method.

The central axis transformation was first proposed by Blum [1], which reconstructs original shape skeleton structures by scanning space with inscribed spheres of varying radii. Building upon this approach, Ramanathan [2] integrated a two-dimensional central axis and surface matching strategy to generate intermediate surfaces. However, for thin-walled structures, redundant feature boundaries tend to induce central axis branching, significantly increasing structural complexity. Additionally, expanding central surface patches is required to generate complete intermediate surfaces, making topological correctness difficult to ensure. Kong et al. [3] proposed an implicit reconstruction method for central axes by combining the central axis field with the directed signed distance field.

The string axis transformation was proposed by Shimada [4], which simplifies tetrahedral meshes into two-dimensional discrete mid-surface meshes through a string surface contraction process. However, this method also struggles to maintain global continuity of mid-surface and stable topological connectivity.

The surface matching method was proposed by Rezayat [5], which pairs surfaces based on inter-surface distances and adjacency graphs to generate intermediate surfaces. To address pairing failures in complex models, Professor Chen Zhiyang et al. [6] developed a variable-thickness intermediate surface generation method based on matching points, though it exhibits limitations in irregular surfaces and one-to-many surface scenarios. Zhu [7] achieved stable extraction of uniform-thickness intermediate surfaces by constructing virtual boundaries and topological connections, but this approach has not yet considered variable wall thickness conditions.

In the field of mesh methods, Fischer [8] reconstructed NURBS control meshes and combined offsetting with sweeping strategies to generate both uniform and variable-thickness mid-surface surfaces. Christoph [9] employed an iterative shrinkage approach to construct density fields, enabling the mesh to progressively collapse inward and form mid-surface structures. While these methods demonstrate certain adaptability, their output quality remains dependent on mesh discretization accuracy.

3. Method

To achieve automatic mid-plane extraction in variable-thickness thin-walled components, we developed the integrated technical workflow illustrated in Figure 1. The process begins with inputting a thin-walled CAD solid model and constructing its directed symbolic distance field, where local extremum analysis identifies potential mid-plane candidate points. Subsequently, the model

undergoes mid-plane connectivity decomposition using surface matching methods combined with geometric adjacency relationships. For uniform thickness regions, offset surface techniques generate intermediate surfaces; for variable-thickness regions, geometric constraints including thickness consistency and normal orientation symmetry are applied to optimize and filter candidate point sets. Mid-plane boundaries are constructed based on decomposition results, followed by surface fitting using optimized mid-plane point sets to produce final mid-plane models that meet topological integrity and geometric accuracy requirements.

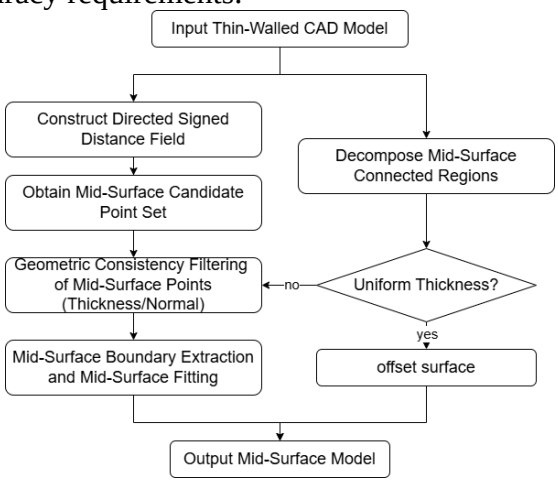

Figure 1: Flowchart of Mid-plane Extraction Algorithm

3.1 Constructing Directed Symbolic Distance Fields

For the input 3D B-Rep geometric model, we first construct its voxelized signed distance field (SDF). The signed distance function is defined as:

$$\phi(x):R^3\rightarrow R \tag{1}$$

Here, x denotes any point in space. The function value $1\phi x$ represents the shortest Euclidean distance from that point to the model boundary. $\phi(x)<0$ indicates the point is located inside the entity; $\phi(x)>0$ indicates the point is located outside the entity; $\phi(x)=0$ corresponds to the model boundary.

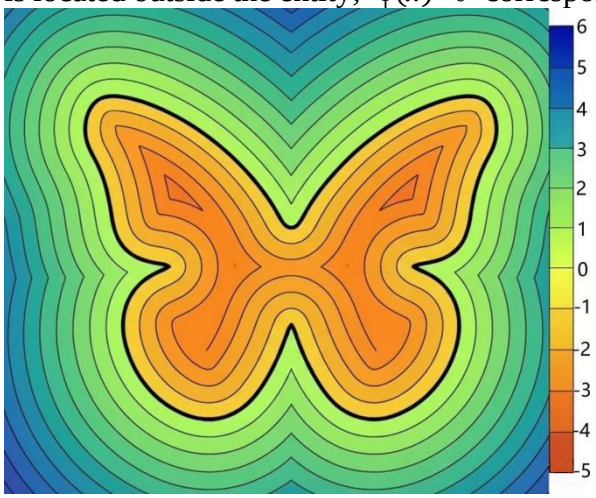

Figure 2 Schematic diagram of two-dimensional directed symbolic distance field

The black solid line in Figure 2 represents the Zero Level Set (ZLS), which corresponds to the actual boundary position of the geometric model. The larger the absolute value, the farther the point

is from the model boundary.

To ensure accurate representation of thin-walled structures and variable thickness regions, an adaptive voxel resolution strategy is employed during the voxelization process. Specifically, voxel dimensions are determined based on the maximum estimated thickness T_{max} obtained from the surface grouping stage described in Section 3.3. The voxel side length Δ is calculated according to the following proportional relationship:

$$\Delta=T_{max}/k \tag{2}$$

Here, k denotes the empirical sampling coefficient, with k=5 adopted in this study.

3.2 Screening of Intermediate Plane Candidate Point Sets

In the constructed directed symbolic distance field, the potential median plane should reside within the entity and correspond to the geometric symmetry center along the local thickness direction. Leveraging this characteristic, we first perform symbolic classification on the distance field voxels, retaining only internal voxel points satisfying $\phi(x)<0$ as the initial candidate set to exclude invalid sampling points from external regions.

To extract potential mid-plane candidate points from internal voxels, this study performs local minimum detection on each internal voxel within the OpenVDB voxel index space. Let the current voxel index be (i, j, k) with corresponding directed symbolic distance field value $\phi_{i,j,k}$. The first-order neighborhood around the voxel is defined as all adjacent voxels satisfying $\Delta i,\Delta j,\Delta k\in\{-1,0,1\}$ that are non-zero simultaneously across x, y, and z directions. If the current voxel satisfies:

$$\phi_{i,j,k}\leq\phi_{i+\Delta i,j+\Delta j,k+\Delta k},\forall(\Delta i,\Delta j,\Delta k)\in\{-1,0,1\}^3\setminus\{(0,0,0)\} \tag{3}$$

The voxel is considered to satisfy the minimization condition within its locally discrete neighborhood and retained as a mid-plane candidate voxel; otherwise, it is excluded.

Through the aforementioned screening process, a set of candidate point sets with mid-plane geometric significance can be extracted from all voxels. These candidate point sets are spatially distributed approximately in the central region of thin-walled structures, effectively limiting the search scope for subsequent mid-plane connectivity decomposition and precise geometric position determination.

3.3 Decomposition of Middle Plane Connectivity Regions

This study is based on a thin-walled recognition method utilizing surface matching. Existing research has demonstrated that this approach exhibits excellent performance in determining the topological range of potential mid-surface locations [10].

For any candidate surface Fi and Fj, we first construct their axis-aligned bounding box (AABB) and perform a coarse screening through bounding box intersection testing to reduce computational complexity.

After passing through the coarse screening process, a surface matching strategy based on normal ray projection is employed to perform discrete sampling on the surface F_i, generating the point set $\{p_k\}$. The normal vector n_k at each sampling point is calculated, followed by ray emission in the antinormal direction to determine the intersection point q_k and distance d_k between the ray and surface F_j. A valid opposing relationship between two surfaces is established when the following conditions are satisfied:

(1) Distance constraint

The maximum normal distance d between two candidate faces must be less than the maximum

thickness t_{max} permitted by the thin-walled solid model.

$$d_{max}<t_{max} \tag{4}$$

The t_{max} value can be either user-defined or determined through statistical analysis of minimum interfacial distances using ray projection calculation models, with the latter being the default setting in this study.

(2) Normal Vector Rule

The normal directions of paired surfaces should be approximately opposite, with their normal dot product satisfying:

$$N1 \cdot N2 <- \varepsilon_n \tag{5}$$

where ε_n denotes the normal tolerance threshold.

When a sampling point meets the aforementioned criteria, it is determined that surfaces F_i and F_j are matched surfaces, and their corresponding thickness values are recorded. If the relative thickness deviation of the recorded thickness value of the ray is less than the thickness threshold (set at 10% in this experiment), the grouping is considered equal thickness; otherwise, it is classified as variable thickness grouping.

Based on the matching surfaces obtained through ray projection and their thickness information, an undirected graph structure can be constructed to record surface-to-surface relationships. In this graph, surface F_i serves as nodes, while matching relationships act as undirected edges. The edge attributes store the inter-surface thickness t_{ij} calculated by ray tracing.

To achieve automatic segmentation of curved surfaces on both sides of the median plane and prevent erroneous merging of thin-walled structures with varying thicknesses, this study introduces a median plane connectivity region decomposition method that combines binary staining strategy with depth-first search (DFS) on matching relationship diagrams. The process is as follows:

First, select any surface in the never visited nodes as the initial node, label it as the A-side surface, and use it as the seed node for current connected domain search. Then, we initiate a depth-first search from this node, expanding the search to all matching adjacent surfaces.

During the traversal process, for each matching edge E_{ij}, in addition to satisfying the topological connectivity condition, a thickness consistency constraint must be introduced. Let the reference thickness of the current connected domain be t_{ref} and the thickness of the matching edge be t_{ij}, with the relative thickness deviation defined as:

$$\delta_t=\frac{|t_{ij}-t_{ref}|}{max(t_{ref},\varepsilon)} \tag{6}$$

When δ_t is less than the preset tolerance threshold τ_t, the matching relationship is considered consistent with the current thin-walled region thickness, allowing inclusion in the same connected domain; otherwise, topological expansion in that direction is terminated. In this study, τ_t=0.1 was adopted.

Under the condition of thickness consistency, binary staining is performed on adjacent surfaces. If the current surface is labeled as Side A, its matching surface is labeled as Side B; conversely, if the current surface is labeled as Side B, its matching surface is labeled as Side A. This process ensures that any matching surface always remains distributed on both sides of the median plane, thereby forming a stable bilateral surface set.

By continuously traversing until no new nodes are added, a complete mid-surface connectivity region can be obtained. Subsequently, all A-side and B-side surfaces within this connectivity domain are classified separately to construct a mid-surface grouping structure, with corresponding regional thickness attributes recorded.

Finally, remove the segmented connected domain nodes from the matching relationship graph and repeat the process until all matched surfaces have completed regional decomposition.

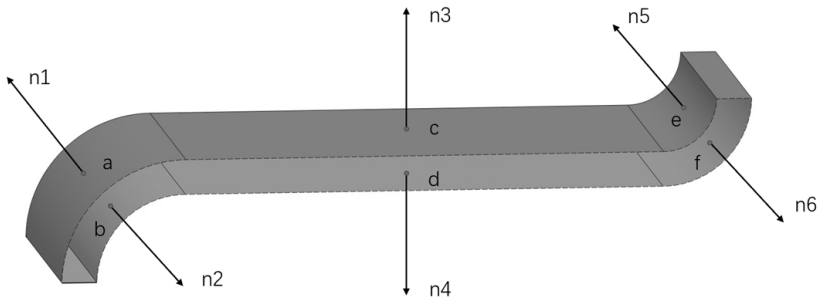

Figure 3: Schematic Diagram of Surface Matching

Based on the aforementioned surface matching results, different paired surfaces form a connected intermediate surface region through topological and geometric constraints, yielding multiple sets of paired surfaces that satisfy normal consistency and constrained inter-surface distances, as illustrated in Figure 3 for the paired surfaces {a, b}, {c, d}, and {e, f}.

This set is utilized to define the spatial scope and boundary conditions of potential thin-walled structures. In the proposed algorithm, it primarily provides a reasonable search domain and geometric constraints for both the candidate surface point set selection in Section 3.4 and boundary extraction in Section 3.5.

3.4 Plane Set in Geometric Consistency Screening

While surface matching and median surface connectivity decomposition can effectively determine the topological extent and boundary conditions of median surfaces, relying solely on the minimum absolute distance between matching surfaces in variable-thickness thin-walled structures still fails to ensure local geometric reliability of median surface points. This limitation primarily stems from the combined effects of thickness discontinuities, surface normal variations, and localized surface matching errors.

To address this, this study employs a directed signed distance field (SDF) as a geometric consistency metric within each mid-plane connectivity region to perform fine-grained screening of mid-plane candidate point sets. It should be noted that the SDF is not used here for direct mid-plane localization, but rather to characterize the local geometric symmetry and stability of candidate points relative to their corresponding thin-walled boundary surfaces.

Specifically, for each candidate point in the mid-surface candidate set, we first estimate the direction from the point to the nearest surface using the SDF gradient information at its location. Then, by integrating the mid-surface connected region associated with the candidate point and its corresponding surface matching relationships, we calculate the point-to-surface distances from all matching surfaces within the region. The pair of matching surfaces with the smallest distances is selected as the local reference surfaces for the candidate point.

To enhance geometric query efficiency, an axis-aligned bounding box (AABB) intersection detection mechanism based on the slab algorithm is implemented during distance calculation and projection processes. This approach enables rapid screening of potential interactive surfaces, effectively reducing the search space for ray-surface intersection queries. It should be emphasized that this acceleration structure is solely designed to improve computational efficiency and does not participate in determining the geometric positions of intermediate planes.

After identifying the local reference surface, perform bidirectional projection along both normal directions (positive and negative) of the candidate point onto adjacent surfaces. The algorithm

calculates the projection distance and the angle between the projection direction and the corresponding surface normal. If any of the following conditions occurs, the candidate point is deemed to fail the mid-plane geometric consistency requirement and will be excluded:

(1) There is significant asymmetry in bidirectional projection distance;

(2) The angle between the projection direction and the normal vector of the corresponding surface exceeds the preset threshold;

(3) The projection distance in either direction exceeds the expected thickness range of the mid-plane region.

By applying the combined constraints of distance symmetry and normal consistency, this approach effectively eliminates unreliable mid-plane candidate points caused by local geometric anomalies or surface matching errors, thereby obtaining a high-quality mid-plane point set that is consistent both topologically and geometrically.

3.5 Mid-plane Boundary Extraction and Intermediate Surface Construction

After completing the extraction of mid-plane candidate points, decomposition of connected regions, and geometric consistency screening, a mid-plane point set with correct topological relationships and relatively stable geometric distribution can be obtained. However, this point set remains essentially discrete sampling points and cannot be directly used as continuous mid-plane representations required for subsequent parametric modeling and geometric analysis. Therefore, it is necessary to further integrate regional boundary information to perform continuous surface reconstruction of the discrete mid-plane point set under boundary constraints.

For regions with uniform thickness, the intermediate surface can be approximated as an equidistant layer between matching surfaces due to minimal local thickness variations, with its boundary position easily determined by corresponding surface boundary relationships. However, in variable-thickness regions where local thickness continuously changes spatially, the intermediate surface no longer satisfies assumptions of fixed offset or simple projection midpoint construction. Direct application of unilateral projection or fixed directional offset methods for intermediate surface construction may lead to positional deviations, boundary discontinuities, or even local distortions caused by directional thickness variations, surface curvature, and unstable matching relationships. Therefore, this study adopts a boundary-constrained surface filling method to reconstruct continuous intermediate surfaces in variable-thickness regions, abandoning direct analytical offset approaches.

Specifically, the mid-plane boundary constraint is first constructed based on the boundary relationships between matching surfaces on both sides of the mid-plane connectivity region. For corresponding surface boundaries near the region boundary, instead of directly calculating midpoints along fixed directions, a virtual boundary reflecting the mid-plane boundary position is established by leveraging the topological correspondence and local geometric distribution of the two-side surface boundaries. This virtual boundary describes the geometric extent and variation trends of the mid-plane within the current connectivity region at the boundary, thereby providing explicit boundary conditions for subsequent mid-plane surface reconstruction.

Meanwhile, the mid-plane candidate points retained after geometric consistency screening are designated as internal geometric constraint points. This point set effectively reflects the spatial distribution of local intermediate layers, with their geometric morphology already refined through thickness consistency, bidirectional projection distance symmetry, and projection angle constraints in previous steps. Consequently, it serves as a reliable basis for internal fitting during continuous mid-plane reconstruction. Thus, mid-plane reconstruction in variable-thickness regions can be conceptualized as: constructing a continuous surface that maximally approximates the mid-plane point set while maintaining overall smoothness, all while satisfying boundary constraints.

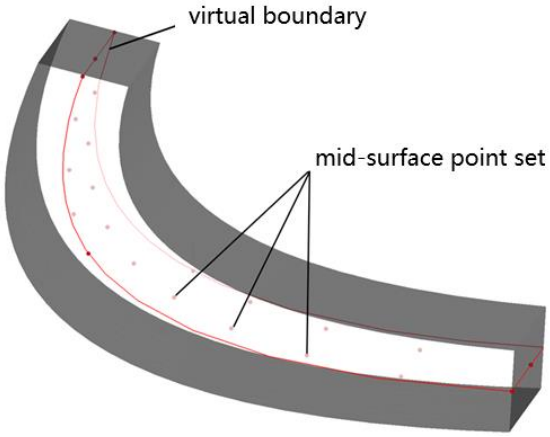

Figure 4 Schematic Diagram of Surface Reconstruction in Variable-thickness Regions based on Virtual Boundaries and Mid-plane Point Sets

As illustrated in Figure 4, this study categorizes the mid-plane reconstruction constraints in variable-thickness regions into two types: virtual boundary constraints derived from matching surface boundary relationships on both sides, and mid-plane point set constraints obtained through geometric consistency screening. The virtual boundaries define the mid-plane's position and topological scope at region boundaries, while the mid-plane point sets characterize the geometric distribution features of local intermediate layers. Since this process does not rely on fixed thickness parameters but instead determines surface morphology through boundary conditions and spatial distribution of candidate points, it demonstrates strong adaptability to scenarios with continuous thickness variations.

In terms of implementation, this study utilizes the BRepFill_Filling class provided by OpenCascade for surface meshing. As a N-sided surface filling algorithm, it generates continuous surfaces by integrating boundary constraints with internal constraints while supporting boundary continuity optimization. During execution, virtual boundaries serve as boundary constraints for surface filling, while the filtered mid-surface point set is incorporated as internal geometric constraints into the meshing process. This approach produces continuous mid-surface surfaces that satisfy regional boundary conditions and approximate the distribution of mid-surface candidate points. It is crucial to note that boundary constraints must be input sequentially to ensure local constraint satisfaction.

It should be noted that the surface filling method employed in this study fundamentally constitutes a continuous surface reconstruction process combining boundary-driven control and point set constraints. For regions with relatively smooth geometric variations, the reconstruction results can effectively approximate the ideal intermediate layer position. In areas with continuous thickness variations or significant curvature changes, virtual boundaries provide boundary topology stability constraints while the mid-plane point set imposes internal geometric distribution constraints. The synergistic interaction between these two mechanisms effectively suppresses mid-plane drift caused by local projection deviations or boundary disturbances, thereby enhancing the stability and continuity of mid-plane reconstruction in variable-thickness regions.

Ultimately, by performing boundary extraction and surface filling on each interconnected region of the mid-surface, we obtain a mid-surface surface that maintains the original thin-walled structure's topological relationships, with continuous boundaries and overall smoothness. This establishes the geometric foundation for subsequent quadric subdivision and volumetric parametric modeling.

4. Implementation and Examples

This study was implemented on Windows 11 (64-bit) platform with hardware configuration including an AMD Ryzen 7 7840HS CPU (3.8GHz) and 32GB RAM. For software development, Visual Studio 2022 was employed as the integrated development environment, utilizing Open Cascade 7.7 for geometric computations and OpenVDB to construct directed symbolic distance fields. The algorithm primarily accepts two input types: thin-walled solid model data and user-specified maximum model thickness.

To validate the effectiveness and robustness of our proposed method, comparative experiments were conducted using multiple thin-walled models with varying wall thickness characteristics, as illustrated in Figure 5. From left to right: the original model, the minimum point set of the directed symbolic distance field, and the generated intermediate surface. Example 1 demonstrates simple one-to-one matching of variable-thickness thin-walled structures; Example 2 shows one-to-one matching of uniform-thickness structures; Example 3 presents one-to-many matching of uniform-thickness structures; and Example 4 illustrates multi-to-many matching of variable-thickness structures. Our method successfully generates intermediate surfaces with high accuracy, demonstrating the algorithm's applicability and reliability for classical thin-walled models.

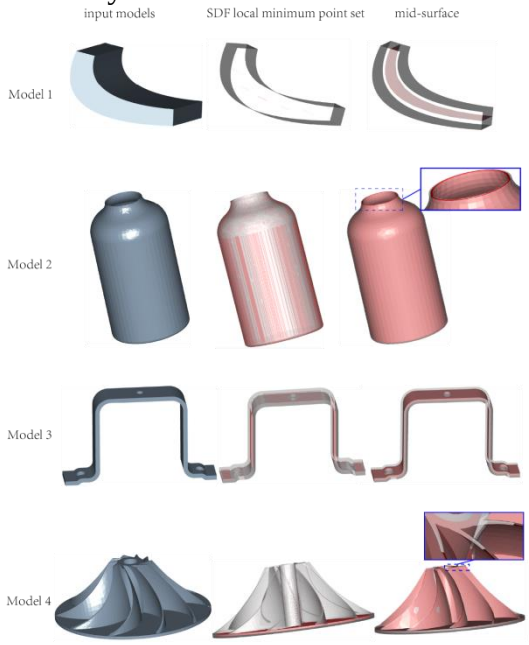

Figure 5: Schematic Diagram of Mid-plane Generation Results for Different Models

Following the qualitative validation of mid-plane reconstruction, quantitative evaluation was further conducted from the perspective of geometric accuracy. The root mean square error (R-error) was adopted as the evaluation metric [11]. Uniform sampling of reconstructed mid-planes was performed to obtain evaluation points, and the distribution proportions across various error intervals were statistically analyzed. The results are presented in Table 1.

Table 1: The Statistical Results for R-errors of Different Benchmarks

R-error	[0,0.1%]	[0.1%,1%]	[1%,10%]	[10%,20%]	[20%,1]
Instance 1	64.57%	35.43%	0	0	0
Instance 2	1	0	0	0	0
Instance 3	1	0	0	0	0
Instance 4	31.27%	62.89%	3.06%	1.96%	0.8%

Statistical results demonstrate that sampling point errors across all instances are predominantly concentrated within the low-error range. Specifically, instances 1-3 maintain errors below 1%, with the majority of sampling points falling below 0.1%. These findings indicate that the proposed method achieves high mid-plane positioning accuracy in both uniform thickness and regular matching structures.

For instance 4 containing complex thickness variations, although over 90% of sampling points still exhibit errors below 1%, a small number of local areas show misregistration points exceeding 1%. Analysis combining with model geometric feature analysis reveals that such errors are primarily distributed in regions with abrupt curvature changes and thickness transition zones.

The comparative analysis of comprehensive diagrams and error statistics demonstrates that the proposed method not only stably extracts mid-plane structures under complex matching relationships at the topological level, but also maintains high geometric accuracy. This validates its effectiveness and robustness in automatic mid-plane extraction tasks for variable-thickness thin-walled components.

5. Conclusion

This study addresses the challenge of automatic mid-plane extraction in variable-thickness thin-walled components by proposing a modeling method that integrates directed symbolic distance fields with surface matching constraints. Research demonstrates that constructing directed symbolic distance fields and extracting local minima effectively characterize the spatial distribution characteristics of neutral layers in thin-walled structures. By combining surface matching relationships with mid-plane connectivity decomposition, the method achieves stable boundary definition of mid-plane topological regions under complex topological conditions. Building upon this foundation, the introduction of joint constraints combining distance symmetry and normal consistency enables geometric consistency screening of mid-plane candidate points, significantly reducing the impact of thickness discontinuities and matching errors on mid-plane localization accuracy.

To address varying thickness configurations, this study employs two distinct strategies: equal-thickness offset generation and variable-thickness boundary-constrained surface fitting, achieving stable transition from implicit mid-plane point sets to explicit mid-plane surfaces. Experimental results demonstrate that the proposed method consistently produces topologically intact mid-plane models with high geometric accuracy across different thickness variation regions, validating the effectiveness of directed signed distance fields in mid-plane localization and stability assessment.

References

[1] BLUM H. A transformation for extracting new descriptions of shape[J]. Models for the perception of speech and visual form, 1967: 362-380.

[2] CHONG C S, KUMAR A S, LEE K H. Automatic solid decomposition and reduction for non-manifold geometric model generation[J]. Computer-Aided Design, 2004, 36(13): 1357-1369.

[3] KONG J, ZONG C, LUO J, et al. Quasi-Medial Distance Field (Q-MDF): A Robust Method for Approximating and Discretizing Neural Medial Axis[J]. arXiv preprint arXiv:2410.17774, 2024.

[4] QUADROS W R, SHIMADA K. Hex-Layer: Layered All-Hex Mesh Generation on Thin Section Solids via Chordal Surface Transformation[C]//IMR. 2002: 169-180.

[5] REZAYAT M. Midsurface abstraction from 3D solid models: general theory and applications[J]. Computer-Aided Design, 1996, 28(11): 905-915.

[6] Chen Zhiyang, Yu Guming, Zhang Yin. Intermediate surface generation of variable wall thickness CAD models based on point matching [J]. China Mechanical Engineering, 2012,23(24):2936-2941+2967.

[7] ZHU H, SHAO Y, LIU Y, et al. Mid-surface abstraction for complex thin-wall models based on virtual decomposition[J]. International Journal of Computer Integrated Manufacturing, 2016, 29(8): 821-838.

[8] FISCHER A, WANG K. (November 1, 1997). A Method for Extracting and Thickening a Mid-Surface of a 3D Thin

Object Represented in NURBS." ASME. J. Manuf. Sci. Eng. November 1997; 119(4B): 706–712. https://doi.org/10.1115/1.2836813
[9] SCHINKO C, ULLRICH T. A new grid-based midsurface generation algorithm[M]//Hyperseeing-The Publication of the International Society of the Arts, Mathematics, and Architecture: Proceedings of SMI'2020 Fabrication and Sculpting Event (FASE). 2020: 81-84.
[10] ZHU H W, SHAO Y L, LIU Y S, ZHAO J J. Automatic hierarchical mid-surface abstraction of thin-walled model based on rib decomposition, Advances in Engineering Software, Volume 97,2016,Pages 60-71,ISSN 0965-9978, https://doi.org/10.1016/j.advengsoft.2016.01.007.
[11] YE L, ZHOU X H, FAN P, TONG R F, LI H L, DU P, TANG M. MidSurfer: Efficient Mid-Surface Abstraction from Variable Thin-Walled Models, Computer-Aided Design, Volume 190,2026,103965,ISSN 0010-4485, https://doi.org/10.1016/j.cad.2025.103965.